The Astrophysical Journal, 802:129 (9pp), 2015 April 1 doi:10.1088/0004-637X/802/2/129

THE EFFECT OF STELLAR MIGRATION ON GALACTIC CHEMICAL EVOLUTION: A HEURISTIC APPROACH

Emanuele Spitoni[1], Donatella Romano[2], Francesca Matteucci[1,3,4], and Luca Ciotti[5]
[1] Dipartimento di Fisica, Sezione di Astronomia, Università di Trieste, Via G.B. Tiepolo 11, I-34143 Trieste, Italy; spitoni@oats.inaf.it
[2] INAF, Osservatorio Astronomico di Bologna, Via Ranzani 1, I-40127 Bologna, Italy
[3] INAF, Osservatorio Astronomico di Trieste, Via G.B. Tiepolo 11, I-34143 Trieste, Italy
[4] INFN, Sezione di Trieste, Via Valerio 2, I-34127 Trieste, Italy
[5] Dipartimento di Fisica e Astronomia, Università di Bologna, Viale Berti-Pichat 6/2, I-40127 Bologna, Italy
Received 2014 September 8; accepted 2015 February 8; published 2015 April 2

ABSTRACT

Stellar migration in Galactic disks has been the subject of several investigations in the past years. However, its impact on the chemical evolution of the Milky Way still needs to be fully quantified. In this paper, we aim to impose some constraints on the significance of this phenomenon by considering its influence on the chemical evolution of the Milky Way thin disk. We do not investigate the physical mechanisms underlying the migration of stars. Rather, we introduce a simple, heuristic treatment of stellar migration in a detailed chemical evolution model for the thin disk of the Milky Way, which already includes radial gas flows and reproduces several observational constraints for the solar vicinity and the whole Galactic disk. When stellar migration is implemented according to the results of chemo-dynamical simulations by Minchev et al. and finite stellar velocities of 1 km s^{-1} are taken into account, the high-metallicity tail of the metallicity distribution function of long-lived, thin-disk stars is well reproduced. By exploring the velocity space, we find that the migrating stars must travel with velocities in the range of 0.5–2 km s^{-1} to properly reproduce the high-metallicity tail of the metallicity distribution. We confirm previous findings by other authors that the observed spread in the age–metallicity relation of solar neighborhood stars can be explained by the presence of stars that originated at different Galactocentric distances, and we conclude that the chemical properties of stars currently observed in the solar vicinity do suggest that stellar migration is present to some extent.

Key words: Galaxy: abundances – Galaxy: disk – Galaxy: evolution – Galaxy: kinematics and dynamics

1. INTRODUCTION

Chemical evolution models are fundamental tools to understand the formation and evolution of the Milky Way (e.g., Matteucci 2001). A good agreement between model predictions and observed properties of the Galaxy is usually obtained by assuming that the disk is well described by concentric annular regions forming by the continuous infall of gas without any exchange of matter between them (e.g., Matteucci & François 1989; Chiappini et al. 1997; François et al. 2004, among many others).

However, in the presence of gas infall, the Galactic disk cannot be adequately described by a model with non-interacting zones (see, e.g., Spitoni & Matteucci 2011, and references therein). In particular, radial motions of gas should be taken into account when the infalling gas has a specific angular momentum lower than that of the matter moving on circular orbits in the disk, so that mixing with the gas in the disk induces a net radial inflow. Lacey & Fall (1985) estimated that the gas inflow velocity is approximately 1 km s^{-1} at 10 kpc. Other internal mechanisms, in principle the ability to induce radial gas flows, may also be present in disk galaxies as a consequence of asymmetric drift (Smet et al. 2014). Goetz & Koeppen (1992), Portinari & Chiosi (2000), Spitoni & Matteucci (2011), Bilitewski & Schönrich (2012), Mott et al. (2013), Spitoni et al. (2013), and Cavichia et al. (2014) present chemical evolution models with the inclusion of radial gas flows. These works generally agree on the magnitude and patterns needed for the gas velocities to fit the observational data: The maximum velocity must not exceed a few km s^{-1}.

On the other hand, in all the models cited above, the stars are assumed to remain at their birth radii. The effect of the interaction of the stars with the spiral arms on the stellar orbits is discussed by Sellwood & Binney (2002), who show that: (a) stars on circular orbits experience larger angular momentum changes and consequently suffer more radial migration than stars on low-angular momentum orbits; (b) stars can migrate to large distances within disks while remaining on nearly circular orbits. By studying the specific case of the Milky Way, Sellwood & Binney (2002) found that old stars formed in the solar neighborhood may have been scattered nearly uniformly within the annular region between 4 and 12 kpc from the Galactic center—a scenario confirmed qualitatively by subsequent studies. For instance, Rŏskar et al. (2008, 2012), using high-resolution *N*-body simulations coupled with smoothed particle hydrodynamics (SPH), have shown that stars can migrate across large Galactocentric distances due to resonant scattering with spiral arms while remaining on almost circular orbits. The spiral perturbations redistribute angular momentum within the disk and lead to substantial radial displacements of individual stars in a manner that largely preserves the circularity of their orbits. These models are able to explain the observed flatness and spread in the age–metallicity relation of solar neighborhood stars. Recent work by Vera-Ciro et al. (2014) confirm that stellar migration can be driven by Sellwood & Binney (2002) corotation scattering process.

The aforementioned dynamical models do not consider the effect of the Galactic bar; the role of the bar for radial migration is thoroughly analyzed in Minchev & Famaey (2010) and Minchev et al. (2011). These authors suggest that radial migration results from the nonlinear coupling between the bar

and the spiral waves, and predict a variation of the efficiency of migration with time and Galactocentric radius. In a more recent study, Halle et al. (2015) confirm that strong radial migration has to be expected in the case of a bar-spiral resonance overlap, but also suggest that the Galactic outer Lindblad resonance acts as a barrier: stars do not migrate from the inner to the outer disk, and vice versa.[6]

Although the existence of the phenomenon of radial migration seems to be established beyond any doubt, a quantitative estimate of its impact on the chemical evolution of the Galactic disk is much more difficult. Besides the aforementioned work of Halle et al. (2015), which challenges any scenario in which significant fractions of stars move from the inner to the outer disk and vice versa, some concerns about the effective role of the bar in stellar migration have been raised by Sánchez-Blázquez et al. (2014). These authors present a comparative study of the stellar metallicity gradients and age distributions in a sample of nearly face-on spiral galaxies, with and without bars. The process of radial migration should flatten the stellar metallicity gradient with time and, therefore, flatter stellar metallicity gradients should be expected in barred galaxies. However, Sánchez-Blázquez and collaborators do not find any difference in the metallicity or in the age gradients of galaxies with or without bars.

The first attempt to analyze the impact that stellar migration could have on the chemical properties of the Milky Way disk was done by François & Matteucci (1993). By discussing the spread observed in the age–metallicity relation and in the [α/Fe] versus [Fe/H] relations for solar neighborhood stars, these authors concluded that most of the observed spread can be accounted for by the fact that some of the stars we observe at the present time in the solar vicinity might have been born in different regions of the Galactic disk, in particular in more inner ones. Their paper was based on observational features of a possible radial migration presented in pioneering works by Grenon (1972, 1989). Grenon identified an old population of super metal-rich stars, which are currently located in the solar vicinity but have kinematics and abundance properties indicative of an origin in the inner Galactic disk.

Despite the recent advances in the field of galaxy formation and evolution, there are currently no self-consistent simulations containing the level of chemical implementation required for making detailed predictions for the number of ongoing and planned Milky Way observational campaigns. Even in high-resolution N-body experiments, one particle represents $\approx 10^{4-5}$ solar masses. Hence, a number of approximations are necessary to compute the chemical enrichment self-consistently inside a dynamical simulation.

Schönrich & Binney (2009a, 2009b) included in a chemical model the radial migration of stars and gas through the disk of the Galaxy by means of a probabilistic approach constrained by Milky Way observables, and found results that were in agreement with Rőskar et al. (2008). They also found that most observational properties and peculiarities of the thick disk could be explained by radial migration. Recently, Minchev et al. (2013, 2014) presented a new approach for combining chemistry and dynamics that overcomes the technical problems originated by fully self-consistent simulations and avoids the star formation (SF) and chemical enrichment problems encountered in previous simulations. They assume that each particle is one star, and implement the SF history and chemical enrichment deriving from a classic chemical evolution model for the thin disk into the simulated Galactic disk. Kubryk et al. (2013, 2014) also studied radial migration and chemical evolution for a general bar-dominated disk galaxy by analyzing the results of a fully self-consistent, high-resolution N-body +SPH simulation. Stars undergo substantial radial migration at all times, caused first by transient spiral arms and later by the bar. The authors stress that, despite the important amount of radial migration occurring in their model, its impact on the chemical properties is limited.

Here, we adopt a phenomenological approach to study the effects of different prescriptions for the stellar migration on the best known chemical evolution observables. In practice, we implement stellar migration in a very simple way, using a detailed chemical evolution model for the Galactic thin disk that already includes radial gas flows. We first focus on the metallicity distribution function of long-lived stars in the solar neighborhood. We then examine the effects of the migration on other observables, such as the age–metallicity relation of stars in the solar vicinity and the stellar density profile across the disk.

The paper is organized as follows: in Section 2 we describe our reference chemical evolution model and the way in which the radial gas flows and the stellar migration have been implemented. In Section 3 we report the model results without stellar migration, while model results with stellar migration are presented in Section 4. Finally, we draw our main conclusions in Section 5.

2. THE CHEMICAL EVOLUTION MODEL

Our reference model for the Galactic thin disk is the one presented in Spitoni & Matteucci (2011). The model assumes that the disk grows via smooth accretion of gas of primordial chemical composition. The infall law is:

$$A(r, t) = a(r)e^{-\frac{t}{\tau_D}}, \quad (1)$$

where τ_D, the e-folding timescale, is a free parameter of the model and the coefficient $a(r)$ is set by the requirement that the current total mass surface density profile of the Galactic thin disk is reproduced. In order to mimic an inside-out formation of the disk (Larson 1976), the timescale for mass accretion is assumed to increase with the Galactic radius following a linear relation (see Chiappini et al. 2001 and references therein):

$$\tau_D(r) = 1.033r\,(\mathrm{kpc}) - 1.27\ \mathrm{Gyr}; \quad (2)$$

this relation holds for Galactocentric distances between 4 and 16 kpc. The region within 4 kpc is not considered in this paper. The infall law adopted in this work is clearly a rough approximation of the true mass assembly history of the disk, which is still necessary because we do not rely on a full cosmological setting. However, it has been shown (Colavitti et al. 2008) that the results of a model assuming such an exponentially decaying infall law are fully compatible with those obtained using cosmological accretion laws.

As for the IMF, we use that of Scalo (1986), which is constant in time and space. We indicate with τ_m the evolutionary lifetime of the stars with initial mass m (Maeder & Meynet 1989). The Type Ia supernova (SN) rate is computed following Greggio & Renzini (1983) and Matteucci

[6] According to Dehnen (2000) the outer Lindblad resonance lies in the vicinity of the Sun.

Table 1
Chemical Evolution Models

Models	τ_D [Gyr]	ν [Gyr^{-1}]	Radial Gas Inflow [km s^{-1}]	Stellar Migration	Stellar Velocities [km s^{-1}]
REF1	1.033 R[kpc]-1.27	Variable (see Figure 1)	1	/	/
REF2	1.033 R[kpc]-1.27	1	1	/	/
"Minchev Case"	1.033 R[kpc]-1.27	Variable	1	10% from 4 kpc	0.5, 1, 2
...	...	(see Figure 1)	...	20% from 6 kpc	...
...	...	...	...	60% from 8 kpc	...

& Greggio (1986). The stellar yields are taken from Woosley & Weaver (1995) for core-collapse supernovae (SNe), van den Hoek & Groenewegen (1997) for low- and intermediate-mass stars, and Iwamoto et al. (1999) for Type Ia SNe. We use an SF rate proportional to the gas surface density:

$$\psi(r, t) \propto \nu \sigma_{\rm gas}^{k}(r, t) \tag{3}$$

where ν is the efficiency of the SF process and $\sigma_{\rm gas}(r, t)$ is the gas surface density at a given position and time. The exponent k is fixed to 1.4 (see Kennicutt 1998).

Motivated by the theory of SF induced by spiral density waves in Galactic disks (Wyse & Silk 1989), we consider a variable star-formation efficiency (SFE) as a function of the Galactocentric distance, $\nu \propto 1/r$ (model REF1, Table 1). This is different from Spitoni & Matteucci (2011), who use a constant value for the SFE (model REF2, Table 1). The reason for this choice is related to the fact that with a constant SFE the predicted abundance ratio patterns (e.g., [O/Fe] versus [Fe/H]) do not change much from radius to radius, thus making the hypothesis of stellar migration as a solution for the observed spread rather unlikely. Figure 1 shows the SFE as a function of the Galactocentric distance used in this work. It is worth emphasizing that a larger SFE in the inner disk is also assumed by Kubryk et al. (2014) and, probably, by Minchev et al. (2013); in the latter paper the authors do not state it explicitly, but an inspection of their results leads us to believe that this is the case. It is the combination of radial migration with a variable SFE across the disk that allows us to reproduce the observed abundance spreads.

2.1. The Implementation of the Gas Radial Flows

In our reference model a constant radial inflow of gas with velocity -1 km s^{-1} is implemented following the prescriptions of Spitoni & Matteucci (2011).

We define the kth shell in terms of the Galactocentric radius r_k, with its inner and outer edge labeled as $r_{k-\frac{1}{2}}$ and $r_{k+\frac{1}{2}}$. We take the inner edge of the k-shell, $r_{k-\frac{1}{2}}$, at the midpoint between the characteristic radii of the shells k and $k-1$, and similarly for the outer edge $r_{k+\frac{1}{2}}$. The flow velocities $v_{k+\frac{1}{2}}$ are assumed to be positive outward and negative inward.

Radial inflows with a flux $F(r)$ contribute to alter the gas surface density σ_{gk} in the kth shell according to

$$\left[\frac{d\sigma_{gk}}{dt}\right]_{rf} = -\frac{F\left(r_{k+\frac{1}{2}}\right) - F\left(r_{k-\frac{1}{2}}\right)}{\pi\left(r_{k+\frac{1}{2}}^2 - r_{k-\frac{1}{2}}^2\right)}, \tag{4}$$

where the gas flow at $r_{k+\frac{1}{2}}$ can be written as

$$F\left(r_{k+\frac{1}{2}}\right) = -2\pi\, r_{k+\frac{1}{2}}\, v_{k+\frac{1}{2}}\, \sigma_{g(k+1)}. \tag{5}$$

We assume that there are no flows from the outer parts of the disk where there is no SF. In our implementation of the radial inflow of gas, only the gas in the Galactic disk at $r < 20$ kpc can move inward by radial inflow.

2.2. Including Stellar Migration in Our Chemical Evolution Model

As discussed in the Introduction, we implement stellar migration in our chemical evolution code using a phenomenological approach, without a specific description of the complex dynamical mechanisms affecting stellar orbits in Galactic disks. In practice, we simply move stars formed at a given radius, with a certain age and a certain metal content, to the solar vicinity, according to some simple rule. Following the work of Kordopatis et al. (2013), we assume as a representative value for the velocity of the stars 1 km s^{-1}, that is, $\simeq$1 kpc Gyr^{-1}. To explore the velocity parameter space, we also run models with stellar velocities fixed to 0.5 and 2 km s^{-1}.

We stress that by taking into account a velocity of 1 km s^{-1}, only stars with stellar lifetimes $\tau_m \geqslant 1$ Gyr, corresponding to initial masses $m \leqslant 2\, M_{\odot}$ (see figure 3 of Romano et al. 2005, and references therein), can travel for distances larger than 1 kpc. We can thus safely assume that most of the metals produced by a stellar generation are ejected well within 1 kpc from their progenitors' birthplace. Therefore, the metal enrichment of the ISM in the solar vicinity is practically unaffected by the stars born in the inner regions, which are thus only "passive tracers" of the process of migration. We notice that, as estimated by Lacey & Fall (1985) with simple calculations, the magnitude of the radial gas flow velocity is roughly 1 km s^{-1} at 10 kpc. Hence, stellar migration and radial gas inflows are characterized by the same timescales, and this is the reason why one has to consider both processes for a complete and consistent study.

First, we want to test the effect of assuming a physically plausible stellar migration on our chemical evolution model predictions. To this aim, we use the results of the chemodynamical simulations by Minchev et al. (2013) to obtain general recipes to use in our pure chemical evolution code. We choose this study because the chemical evolution model adopted by the authors is very similar to ours, which allows us to test of the validity of our approach. Indeed, as we will show in Section 4, if we assume that 10% and 20% of the stars born at 4 and 6 kpc, respectively, migrate toward 8 kpc, while

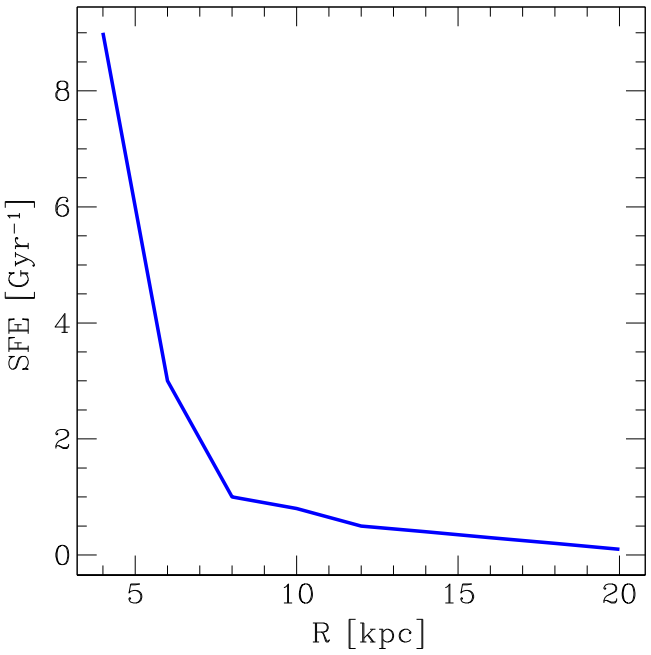

Figure 1. Adopted star-formation efficiency as a function of Galactocentric radius for our models (except model REF2, which assumes a constant star-formation efficiency).

60% of those born at 8 kpc leave the solar neighborhood (percentages are drawn from Minchev et al.'s dynamical simulations), the metallicity distribution function we predict for long-lived solar vicinity stars turns out to be very similar to that obtained by Minchev and collaborators.

We also test some extreme cases that are not supported by dynamical studies, with the aim of exploring the effects that a huge migration of stars would have on the chemical evolution of the solar neighborhood (see Section 4).

3. MODEL RESULTS WITHOUT STELLAR MIGRATION

In this section, we present the results of our chemical evolution model including radial gas flows, either with variable (model REF1) or constant SFE (model REF2).

In Table 1, the principal characteristics of the models are reported: the timescale of thin-disk formation, τ_D, is listed in column 2; the adopted SFEs in column 3; and the velocity of the radial gas inflow in column 4. For the model including stellar migration ("Minchev case" model), columns 5 and 6 specify the adopted prescriptions about the fraction of migrating stars and their velocities.

In Figure 2 it is shown that model REF1 (red curve, labeled 13 Gyr) perfectly fits the present-day oxygen abundance gradient measured in Cepheids. The data (from Luck & Lambert 2011) have been divided into bins 1 kpc wide; for each bin we compute the average value and the relative standard deviation. In Figure 2 we also show the evolution of the gradient, computed at 4, 6, 8, and 13 Gyr. It is worth noting that the combination of a variable SFE—with higher values in the inner-disk regions—with a constant radial gas flow leads to a steepening of the gradient in time.

In the upper panel of Figure 3 we show the [O/Fe] versus [Fe/H] relations obtained with model REF1 at different Galactocentric distances, spanning the range between 4 and 16 kpc. The theoretical predictions are very similar to those reported by Minchev et al. (2013; see their Figure 4, bottom left panel) and are mainly driven by the adoption of an SFE that varies with the Galactocentric distance in the model. For reference, we also plot data for solar neighborhood thin-disk stars by Bensby et al. (2005). In the lower panel of Figure 3 we show the effects of assuming a constant SFE (model REF2) on the [O/Fe] versus [Fe/H] diagram. It is immediately seen that the observed spread in the data can not be reproduced by the chemical evolution model. We conclude that the hypothesis of stellar migration as a solution for the observed spread requires a variable SFE. This is even more evident from Figure 4, where we show the age–metallicity relation predicted by model REF1 for different Galactocentric distances, compared to the data for thin-disk stars in the solar vicinity from Bensby et al. (2014). Other authors have already claimed (e.g., François & Matteucci 1993; Schönrich & Binney 2009a) that the observed spread in the data can be explained with the migration of stars both from the inner and the outer regions, and we confirm their findings. Also, we remark that, while the migration produces a spread of up to 1 dex in [Fe/H] at a given age, a much lower spread is expected in the [O/Fe] ratios at a given metallicity (see Figures 3 and 4), which is in agreement with what is suggested from the observations (see Edvardsson et al. 1993, who first discussed the conundrum of a large spread in the age–metallicity relation apparently contrasting with the tightness of the [element/Fe] versus [Fe/H] relations for solar neighborhood stars).

In Figure 5 we compare the metallicity distribution function of long-lived, thin-disk stars predicted by model REF1 (dashed line) to the observed ones from Adibekyan et al. (2013; solid histogram) and Fuhrmann (2011; dashed histogram). The sample of Adibekyan et al. (2013), comprising stars with Galactocentric distances between 7.9 and 8.1 kpc, with heights above the Galactic plane $|Z|$ smaller than 0.1 kpc, is not a pure thin-disk sample. However, thin-disk stars can be separated from the rest of the sample based on a chemical criterion (the [α/Fe] versus [Fe/H] plot; see Adibekyan et al. 2013). The distributions of Adibekyan et al. (2013) and Fuhrmann (2011), while agreeing on the position of the peak, significantly differ in shape. This could be due to sample selection effects: While Fuhrmann's survey is limited to objects with *Hipparcos* data within 25 pc from the Sun, Adibekyan et al. (2013) rely on high-resolution analysis of a kinematically unbiased sample of more than 1000 FGK stars located up to 600 pc—but mostly within 50 pc—from the Sun. Interestingly, the APOGEE distribution, extending to significantly larger distances and sampling nearly 10 times more stars, compares well to that from Adibekyan et al. (2013; see Anders et al. 2014). Therefore, in the following we will use the Adibekyan et al. (2013) distribution for comparison with the model predictions. We also recall that our Galactic chemical evolution model is a "sequential" one, and that we consider as thin-disk stars only those with [Fe/H] $\geqslant -0.6$ dex. We see that the metallicity distribution function of Adibekyan et al. (2013) is fairly well reproduced by our model with radial gas inflow and no stellar migration. However, we note that the model underestimates the high-metallicity tail of observed distribution. In Figure 5, the theoretical and observed metallicity distribution functions are normalized to the corresponding maximum number of stars for each distribution. If we normalize the distributions to the total number of stars (see Figure 6, left panel), a good agreement is still found between model predictions and observations.

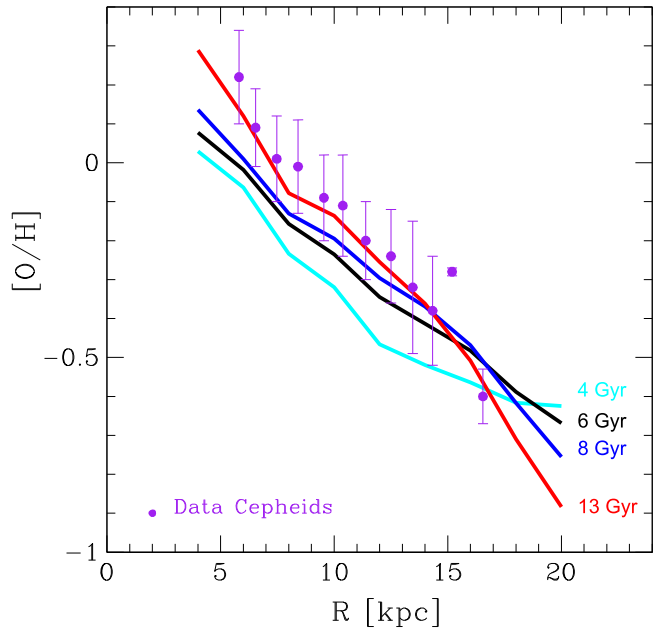

Figure 2. Evolution in time of the oxygen abundance gradient along the Galactic disk for our reference model in the presence of radial gas flows and variable star-formation efficiency (model REF1); shown are the predictions of the model at 4, 6, 8, and 13 Gyr. The model results are compared to data from Cepheids (Luck & Lambert 2011), which track the present-day gradient.

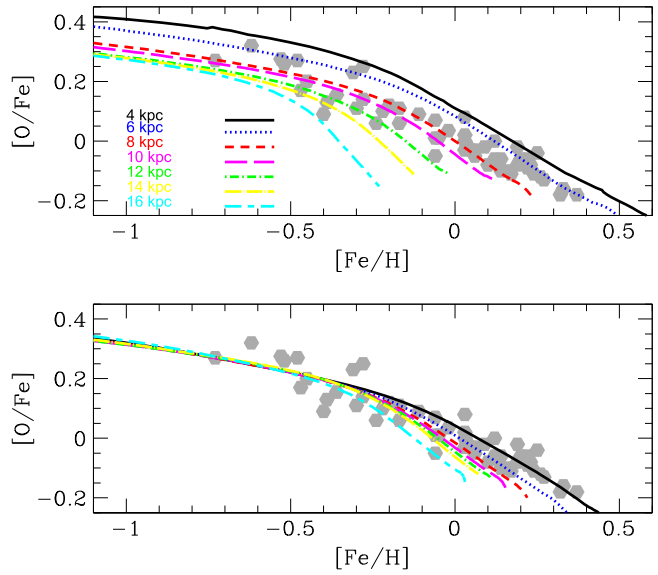

Figure 3. [O/Fe] vs. [Fe/H] relations (lines) predicted by our models REF1 (upper panel) and REF2 (lower panel) at different Galactocentric distances, as indicated in the bottom left legend in the top panel. The two models include radial gas flows and differ only in the assumed SFE (see text). The data (symbols in both panels) refer to solar neighborhood thin-disk stars and are taken from Bensby et al. (2005).

In Figure 7 we show the G-dwarf metallicity distributions obtained by model REF1 at 4, 6, and 8 kpc distance from the Galactic center. As expected, the relative number of high-metallicity stars increases going toward the Galactic center, due to the faster evolution and more efficient SF in the inner regions. These predictions can be compared to data from large spectroscopic surveys, such as APOGEE and *Gaia*-ESO, which are mapping increasingly larger volumes of the Milky Way disk (e.g., $5 < R < 11$ kpc, $0 < |Z| < 2$ kpc, Nidever et al. (2014)—APOGEE; $4 < R < 12$ kpc, $0 < |Z| < 3.5$ kpc, Mikolaitis et al. 2014—*Gaia*-ESO Survey).

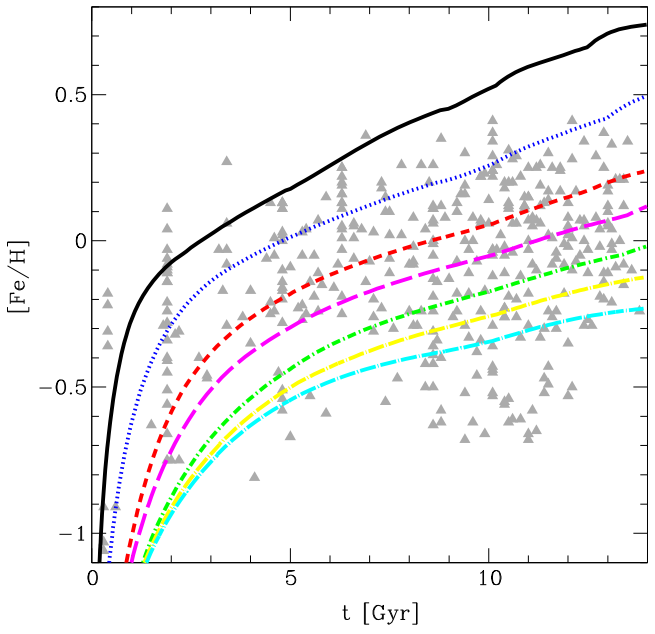

Figure 4. Temporal evolution of [Fe/H] for our best model REF1 with radial gas flows and variable SFE at different Galactocentric distances (curves; see Figure 3, upper panel, for the legend). Also shown are data by Bensby et al. (2014) for solar neighborhood stars (symbols).

Finally, in Figure 8, the current stellar surface density profile predicted by model REF1 is reported as a black solid line. To compare our model predictions with the relevant data (yellow stripe in the plot), we consider a local stellar density of $35 \pm 5\, M_{\odot}\, \mathrm{pc}^{-2}$ (Gilmore et al. 1989) and assume that the stellar profile decreases exponentially outward with a characteristic length scale of 2.5 kpc (Sackett 1997).

We stress that all the abundance ratios presented in this section are normalized to our theoretical solar abundances, namely the abundances predicted in the ISM at 8 kpc 4.5 Gyr ago. In Section 4 we will use the same normalization.

4. MODEL RESULTS IN THE PRESENCE OF STELLAR MIGRATION

We now illustrate the results of the models that include radial stellar migration. First, we set some simple rules to make stars travel across the disk, somehow mimicking the results of more complex, self-consistent chemo-dynamical models (Minchev et al. 2013): we assume that 10% of the stars born at 4 kpc and 20% of those born at 6 kpc migrate toward 8 kpc, whereas 60% of those born in the solar neighborhood migrate (both outwards and inwards); the migrating stars have a velocity of 1 km s^{-1}. We refer to this model as the "Minchev case" model (see Table 1). The metallicity distribution function of long-lived solar neighborhood stars obtained with this model is reported in Figure 9 (red solid line). It is clear that we are now able to explain not only the peak and left wing of the observed distribution (magenta histogram; Adibekyan et al. 2013), but also its high-metallicity tail. We also show in Figure 9 the separate contributions of stars born at 4 and 6 kpc that end up in the solar neighborhood (green dotted–dashed and blue dashed lines, respectively), as well as that of stars born in situ (light blue dashed line). By comparing this figure with Figure 3

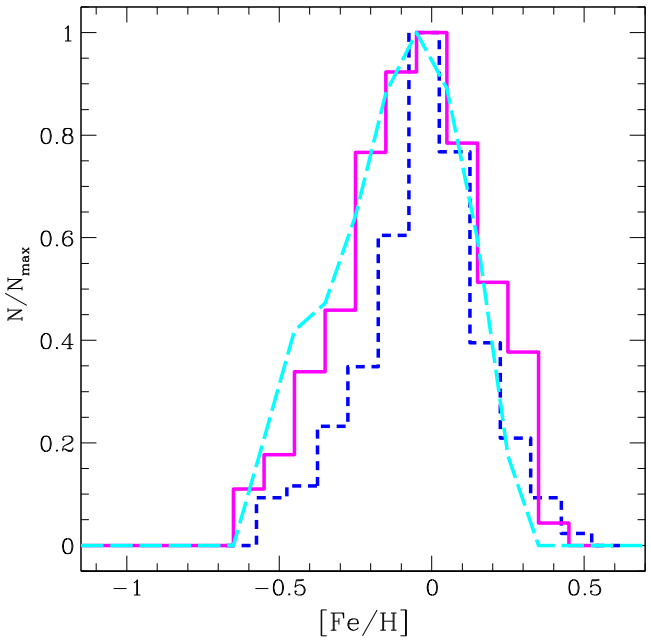

Figure 5. The G-dwarf metallicity distribution predicted by model REF1 (dashed line), which does not include stellar migration but includes a constant radial gas inflow of 1 km s^{-1}, is compared to the observed distributions of thin-disk stars by Adibekyan et al. (2013; solid magenta histogram) and Fuhrmann (2011; short-dashed blue histogram).

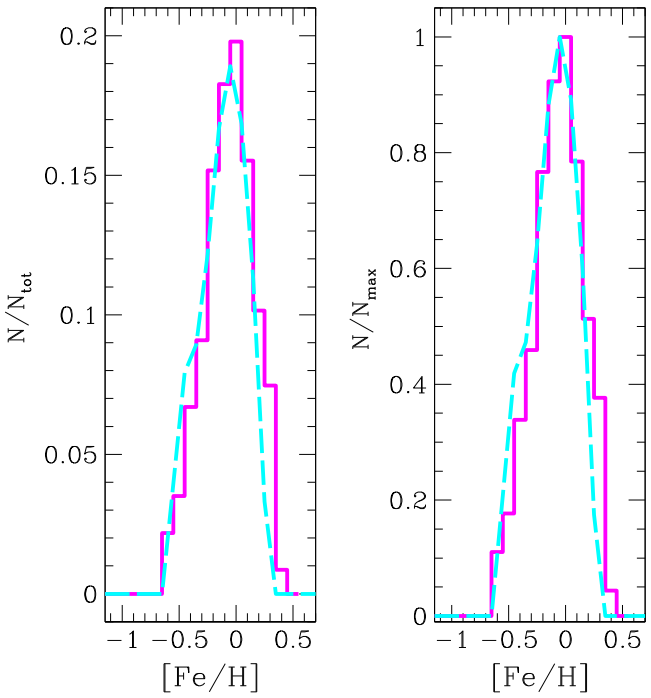

Figure 6. The G-dwarf metallicity distribution predicted by model REF1 without stellar migration (dashed line) is compared to the one observed by Adibekyan et al. (2013; solid histogram). The distributions are normalized to either the total or the maximum number of stars in each distribution (left and right panels, respectively).

(middle panel) of Minchev et al. (2013), we note that our model is entirely consistent with their results in terms of the G-dwarf metallicity distribution. The stellar surface density profile that is obtained with the above prescriptions for stellar migration is presented in Figure 8 (green dashed line). The

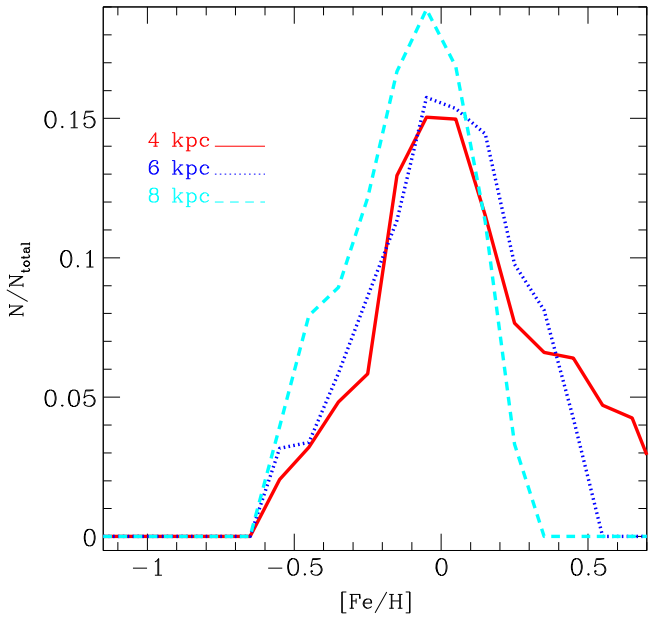

Figure 7. The G-dwarf metallicity distributions predicted by model REF1 at 4, 6, and 8 kpc, assuming radial gas flows and no stellar migration.

observed profile (yellow stripe) is reproduced and the model leads to a stellar surface density of 33 $M_{\odot}$ pc^{-2} in the solar neighborhood, which is in agreement with the observed value.

In Figure 10, we explore the effects of different assumptions about the velocities of the migrating stars on the predicted G-dwarf metallicity distribution (the stars migrate according to the scheme discussed in the previous paragraph). We either do not take the stellar velocity into account, or analyze cases in which stellar velocities of 0.5, 1, and 2 km s^{-1} are considered. The observed G-dwarf metallicity distribution is best reproduced with a velocity of 1 km s^{-1}. Adopting a smaller velocity (e.g., 0.5 km s^{-1}) has the consequence that many more stars among those born more recently and at larger distances from the solar neighborhood have not had sufficient time to reach the solar vicinity, compared to models that assume larger stellar velocities. As a result, the right tail of the Adibekyan et al. (2013) distribution is no longer reproduced, and the model tends to the case without stellar migration.

Kobayashi & Nakasato (2011) presented chemo-dynamical simulations of a Milky Way–type galaxy using a self-consistent hydrodynamical code that includes SN feedback and chemical enrichment, and predicts the spatial distribution of elements from oxygen to zinc. With their model they predict that only 30% of the stars that reside in the solar neighborhood have originated from different regions of the Galactic disk (C. Kobayashi 2015, private communication). In Minchev et al. (2013), approximately 60% of the stars currently found in the solar neighborhood would have formed at 4 and 6 kpc. Therefore, so far, it is not possible to reach firm conclusions about the effective amount of stellar migration in the Galactic disk. It is interesting to note, as already pointed out by previous authors, that stellar migration brings to the solar neighborhood a few old, metal-rich stars, thus fulfilling the requirements implied by observations of Grenon (1972, 1989). However, it is also important to stress that it does not lead to substantial changes in the theoretical metallicity distribution function of long-living stars, making a quantification of the extent of migration based on this observable a hard task.

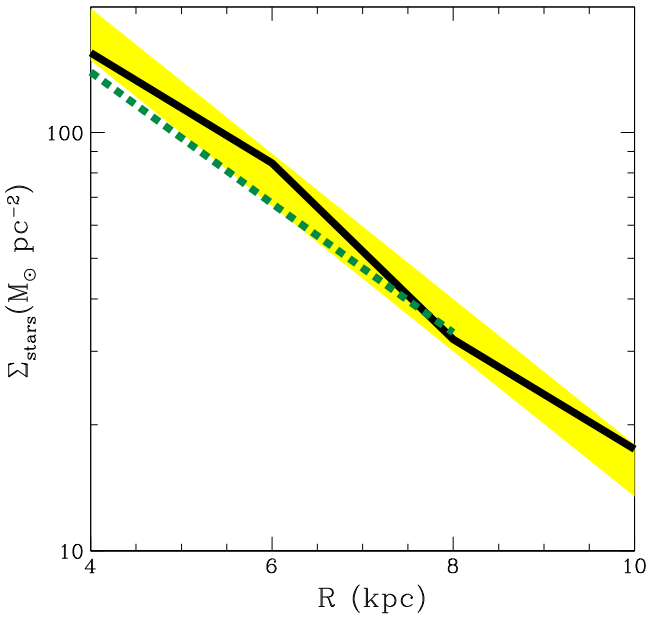

Figure 8. The stellar surface density profile predicted by the chemical evolution model REF1 is shown as a black solid line. The green dashed line represents a model in which stellar migration is included according to the results of chemo-dynamical simulations by Minchev et al. (2013; model labeled "Minchev case" in Table 1): 10% (20%) of the stars born at 4 kpc (6 kpc) move toward 8 kpc, whereas 60% of the stars born at 8 kpc leave the solar neighborhood. The yellow stripe indicates the area spanned by the observational data (see text).

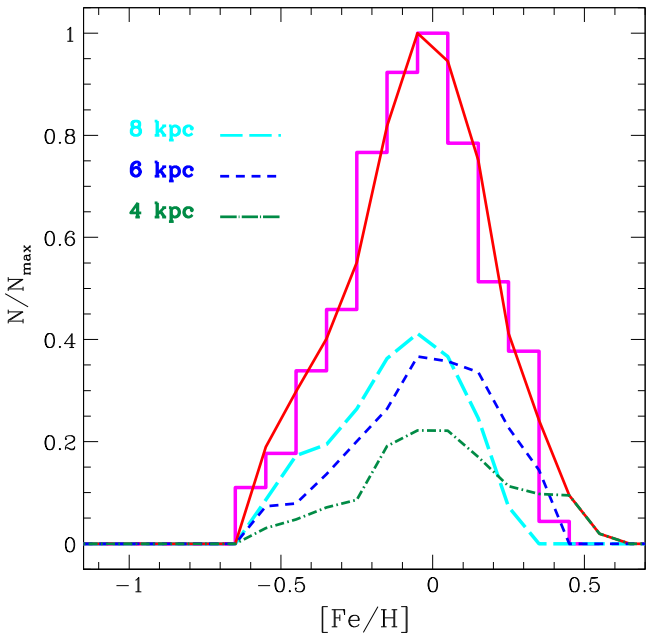

Figure 9. Red solid line: theoretical G-dwarf metallicity distribution obtained with the "Minchev case" model, which assumes radial gas flows and stellar migration according to the following recipe: 10% and 20% of the stars born at 4 and 6 kpc, respectively, move toward 8 kpc, whereas 60% of the stars born in situ leave the solar neighborhood; the stars are assigned a velocity of 1 km s^{-1}. The contributions of the stars born at different Galactocentric radii are also shown (legend on top left corner). The data (magenta histogram) are from Adibekyan et al. (2013).

Another important issue is that the migrated stars could end up populating the thick disk in the solar neighborhood, as indicated by Minchev et al. (2013): in this case, the G-dwarf

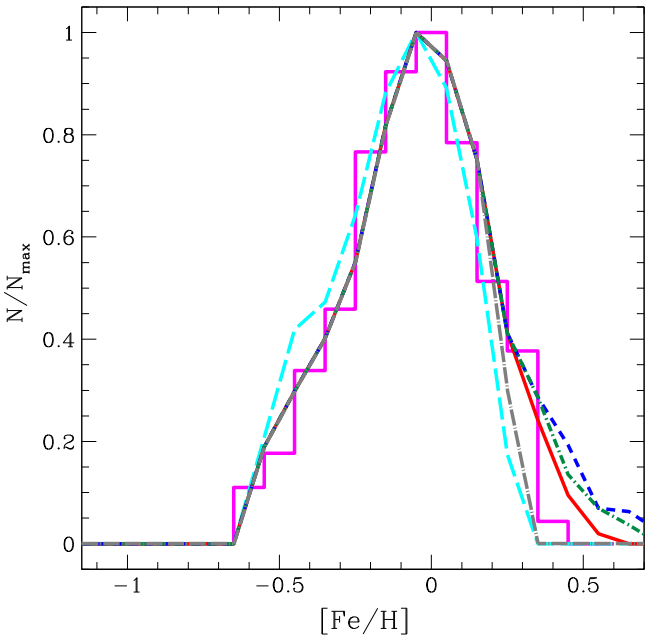

Figure 10. Effects of different prescriptions about the velocity of the migrating stars on the metallicity distribution of solar neighborhood long-lived stars predicted with the "Minchev case" model. The short-dashed blue line represents the model results when the finite velocity of the stars is not taken into account. The solid red and short-dashed–dotted green lines refer to adopted velocities of 1 and 2 km s^{-1}, respectively, while the long-dashed–dotted gray line stands for a case in which the stellar velocity is set to 0.5 km s^{-1}. With the long-dashed cyan line we also show our reference model (REF1) without stellar migration. The data (magenta histogram) are for thin-disk stars from Adibekyan et al. (2013).

metallicity distribution would suffer an even smaller effect by migrating stars.

We compute the numbers of stars in the solar neighborhood that are expected to have a given [O/Fe] at a given [Fe/H], as well as the numbers of stars with a certain [Fe/H] at a given age, for the "Minchev case" model taking into account a stellar velocity of 1 km s^{-1} (see Figures 11 and 12, respectively). Figure 12 clearly shows the effect of setting the velocity of the stars to a fixed value. We are considering velocities fixed at 1 km s^{-1} $\approx$ 1 kpc Gyr^{-1} and, thus, the curve relative to the stars coming from 4 kpc ends at 10 Gyr: all stars born at 4 kpc at times larger than 10 Gyr from the beginning of the simulation do not have enough time to reach the solar neighborhood. The same explanation is valid for the 6 kpc line result (i.e., for times larger than 12 Gyr no stars formed at 6 kpc can reach the solar neighborhood).

In Figure 13, we show the metallicity distributions of long-lived stars in the solar vicinity predicted by our models with (dashed lines; "Minchev case" model, velocity of the migrating stars set to 1 km s^{-1}) and without stellar migration (solid lines; model REF1). The total distributions (cyan lines) are split into different age bins: we consider young stars (ages $<$ 1 Gyr; blue lines), intermediate-age stars (1 Gyr $<$ ages $<$ 5 Gyr; black lines), and old stars (ages $>$ 5 Gyr; red lines). Each distribution is normalized to the total number (young+intermediate+old) of stars. The finite velocity of the stars is taken into account in order to establish how many inner-disk stars end up in the solar neighborhood.

In our reference model without stellar migration (model REF1, with variable SFE and radial gas inflow included with a velocity of 1 km s^{-1}), 3.30% of the stars present ages less than 1 Gyr, 23.74% have ages between 1 and 5 Gyr, and

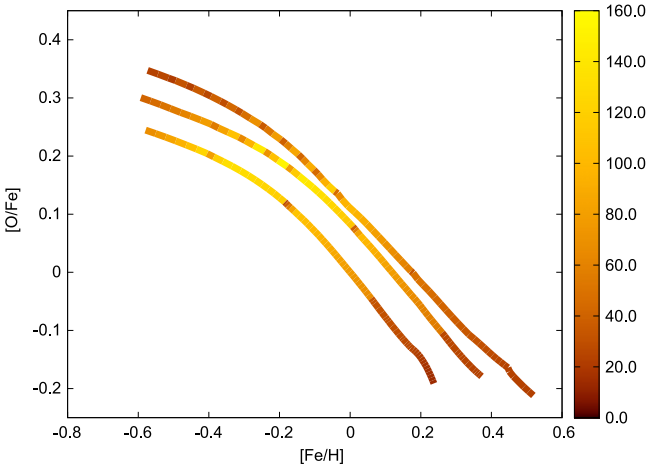

Figure 11. [O/Fe] vs. [Fe/H] in the solar neighborhood for the "Minchev case" model, where a velocity of 1 km s^{-1} is considered for the migrating stars. The lines are color-coded according to the number of stars (in unit of 10^6). The upper curve refers to stars born at 4 kpc, the middle one to stars born at 6 kpc, and the lower curve represents stars born in situ.

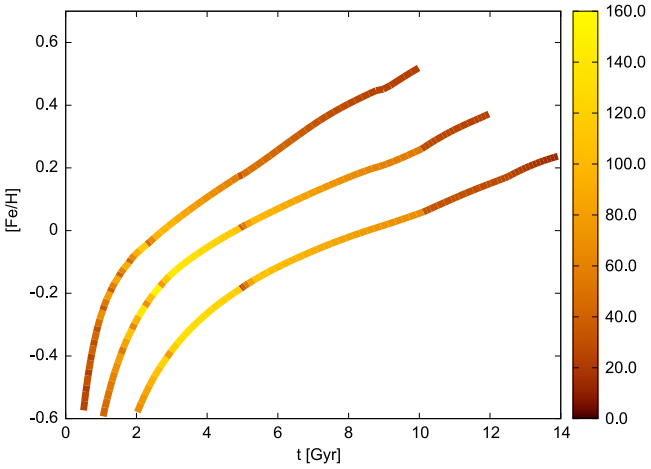

Figure 12. [Fe/H] vs. time in the solar neighborhood for the "Minchev case" model, where a velocity of 1 km s^{-1} is considered for the migrating stars. The lines are color-coded according to the number of stars (in unit of 10^6). The upper curve refers to stars born at 4 kpc, the middle one to stars born at 6 kpc, and the lower curve represents stars born in situ.

the oldest stars (larger than 5 Gyr) are 72.96% of the total. Concerning the model with stellar migration ("Minchev case" model), 1.25% of the stars have ages less than 1 Gyr, 15.93% have ages between 1 and 5 Gyr, and the oldest stars with ages larger than 5 Gyr are 82.82%. Different prescriptions for the stellar velocities would increase (smaller velocities) or decrease (larger velocities) the contribution of the old stars to the G-dwarf metallicity distribution function. The main effect of the stellar migration, in the way in which it is implemented here, is to increase the percentage of old stars in the solar neighborhood compared to the model without stellar migration.

Finally, we test the effects on the metallicity distribution of long-lived stars in the solar neighborhood of "extreme" stellar migrations, where we do not allow stars born in situ at 8 kpc to migrate toward other regions. We distinguish three cases:

1. Case (1): 10% of the stars born at 4 kpc and 20% of those born at 6 kpc migrate toward 8 kpc;

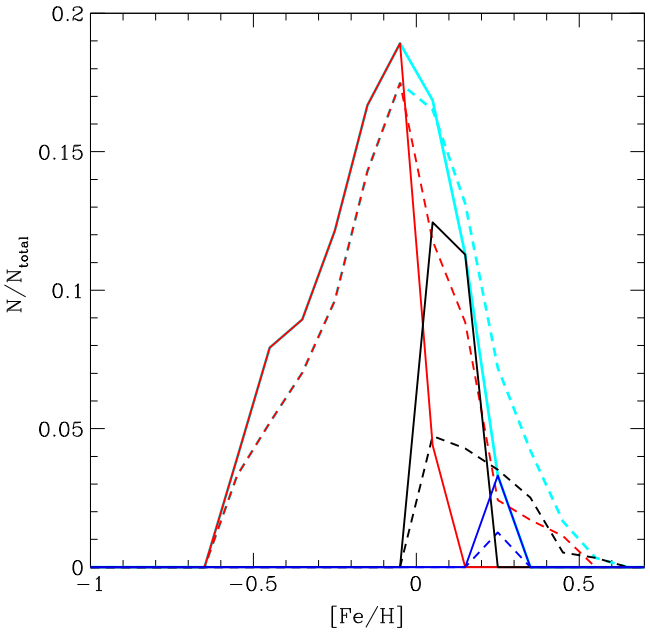

Figure 13. G-dwarf metallicity distributions at 8 kpc obtained by our models for young stars (ages < 1 Gyr; blue lines), intermediate-age stars (1 Gyr < ages < 5 Gyr; black lines), and old stars (ages > 5 Gyr; red lines). The cyan lines show the sum of all age distributions. The solid lines refer to model REF1, without stellar migration but including radial gas flows. The dashed lines refer to the "Minchev case" model with velocity of the migrating stars fixed at 1 km s^{-1}. Each distribution is normalized to the total number (young+intermediate+old) of stars.

2. Case (2): 20% of the stars born at 4 kpc and 40% of those born at 6 kpc migrate toward 8 kpc;
3. Case (3): all the stars born at 4 and 6 kpc migrate toward 8 kpc.

We show (Figure 14) that the main effect of stellar migration in these extreme cases (even in the really extreme and unphysical case 3) is to populate the high-metallicity tail of the predicted distribution. Overall, the predicted stellar metallicity distribution is not substantially affected. In particular, the position of the peak is left unchanged: it mostly depends on the assumed timescale of thin-disk formation. We conclude that the G-dwarf metallicity distribution cannot be used to extract information on the extent and significance of stellar migration. However, this process is clearly needed in order to improve the agreement between model predictions and observations on the high-metallicity tail.

5. CONCLUSIONS

In this paper we have studied the effects of the stellar migration by means of a detailed chemical evolution model where radial gas flows in the Galactic disk are also considered. The stellar migration is implemented in the code in a phenomenological way, just mimicking the results of published dynamical models, with no intention of studying the physics of this phenomenon. Our main conclusions can be summarized as follows:

1. Our reference chemical evolution model for the thin disk of the Milky Way—assuming a variable SFE, a constant radial gas inflow (fixed at −1 km s^{-1}), and no stellar migration—is able to fit well the majority of the observables: the abundance gradient along the Galactic

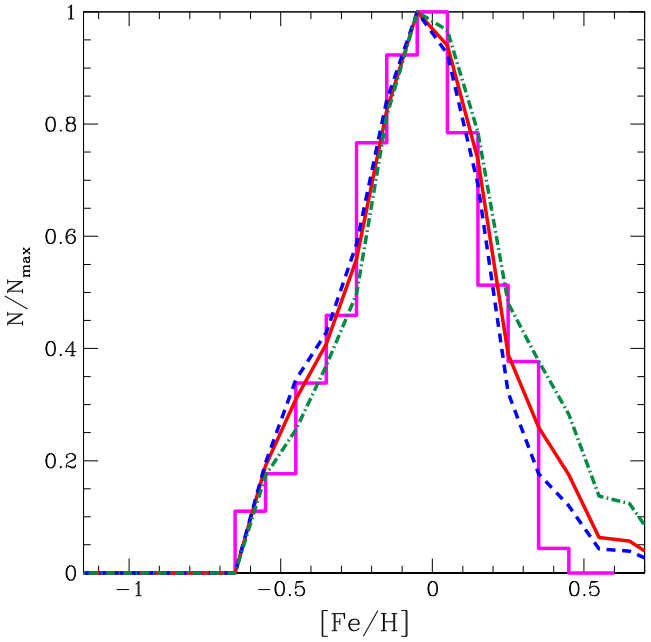

Figure 14. G-dwarf metallicity distributions predicted by our "extreme" models where stars born in situ at 8 kpc are not allowed to migrate. The dashed blue line refers to the predictions of case (1) migration (10% and 20% of the stars born at 4 and 6 kpc, respectively, end up at 8 kpc). Case (2) migration (20% and 40% of the stars born at 4 and 6 kpc, respectively, end up at 8 kpc) is represented by the solid red line, and case (3) migration (all stars born at 4 and 6 kpc end up at 8 kpc) is represented by the green dashed–dotted line. The observed distribution of thin-disk stars (magenta histogram) is taken from Adibekyan et al. (2013).

disk and the stellar mass surface density profile. In addition, the observed G-dwarf metallicity distribution of thin-disk stars (Adibekyan et al. 2013) is generally in agreement with our model, with the only problem residing in the high-metallicity tail of the distribution, which our model is underestimating.

2. By including stellar migration according to simple prescriptions that mimic the results of chemo-dynamical models by Minchev et al. (2013), and taking into account velocities of 1 km s^{-1} for the migrating stars, we are able to reproduce very well the high-metallicity tail of the G-dwarf metallicity distribution observed for thin-disk stars.
3. By exploring the velocity space, we conclude that the stellar migration velocities must have values larger than 0.5 km s^{-1} and smaller than 2 km s^{-1} to properly reproduce the high-metallicity tail in the G-dwarf metallicity distribution of thin-disk stars.
4. As found by previous authors (François & Matteucci 1993; Schönrich & Binney 2009a; Minchev et al. 2013) the observed spread, if real, in [O/Fe] versus [Fe/H], and age versus [Fe/H] relations, can be partially explained by taking stellar migration into account. We proved that the hypothesis of stellar migration as a solution for the observed spread requires a variable SFE.

We thank the anonymous referee for the suggestions that improved the paper. We acknowledge financial support from PRIN MIUR 2010-2011, project "The Chemical and Dynamical Evolution of the Milky Way and Local Group Galaxies," Prot. 2010LY5N2T.

REFERENCES

Adibekyan, V. Zh., Figueira, P., Santos, N. C., et al. 2013, A&A, 554, A44
Anders, F., Chiappini, C., Santiago, B. X., et al. 2014, A&A, 564, A115
Bensby, T., Feltzing, S., Lundstrom, I., & Ilyin, I. 2005, A&A, 433, 185
Bensby, T., Fetzing, S., & Oey, M. S. 2014, A&A, 562, A71
Bilitewski, T., & Schönrich, R. 2012, MNRAS, 426, 2266
Cavichia, O., Mollá, M., Costa, R. D. D., & Maciel, W. J. 2014, MNRAS, 437, 3688
Chiappini, C., Matteucci, F., & Gratton, R. 1997, ApJ, 477, 765
Chiappini, C., Matteucci, F., & Romano, D. 2001, ApJ, 554, 1044
Colavitti, E., Matteucci, F., & Murante, G. 2008, A&A, 483, 401
Dehnen, W. 2000, AJ, 119, 800
Edvardsson, B., Andersen, J., Gustafsson, B., et al. 1993, A&A, 275, 101
François, P., & Matteucci, F. 1993, A&A, 280, 136
François, P., Matteucci, F., Cayrel, R., et al. 2004, A&A, 421, 613
Fuhrmann, K. 2011, MNRAS, 414, 2893
Gilmore, G., Wyse, R. F. G., & Kuijken, K. 1989, ARA&A, 27, 555
Goetz, M., & Koeppen, J. 1992, A&A, 262, 455
Greggio, L., & Renzini, A. 1983, A&A, 118, 217
Grenon, M. 1972, in IAU Coll. 17, Age des Etoiles, ed. G. Cayrel de Strobel, & A. M. Delplace (Meudon: Observatoire de Paris), 55
Grenon, M. 1989, Ap&SS, 156, 29
Halle, A., Di Matteo, P., Haywood, M., & Combes, F. 2015, A&A, submitted (arXiv:1501.00664)
Iwamoto, K., Brachwitz, F., Nomoto, K., et al. 1999, ApJS, 125, 439
Kennicutt, R. C., Jr. 1998, ApJ, 498, 541
Kobayashi, C., & Nakasato, N. 2011, ApJ, 719, 16
Kordopatis, G., Gilmore, G., Steinmetz, M., et al. 2013, AJ, 146, 134
Kubryk, M., Prantzos, N., & Athanassoula, E. 2013, MNRAS, 436, 1479
Kubryk, M., Prantzos, N., & Athanassoula, E. 2014, A&A, submitted (arXiv:1412.0585)
Lacey, C. G., & Fall, M. 1985, ApJ, 290, 154
Larson, R. B. 1976, MNRAS, 176, 31
Luck, R. E., & Lambert, D. L. 2011, AJ, 142, 136
Maeder, A., & Meynet, G. 1989, A&A, 210, 155
Matteucci, F. 2001, The Chemical Evolution of the Galaxy, Vol. 253 (Dordrecht: Kluwer)
Matteucci, F., & François, P. 1989, MNRAS, 239, 885
Matteucci, F., & Greggio, L. 1986, A&A, 154, 279
Mikolaitis, Š, Hill, V., Recio-Blanco, A., et al. 2014, A&A, 572, A33
Minchev, I., Chiappini, C., & Martig, M. 2013, A&A, 558, A9
Minchev, I., Chiappini, C., & Martig, M. 2014, A&A, 572, A92
Minchev, I., & Famaey, B. 2010, ApJ, 722, 112
Minchev, I., Famaey, B., Combes, F., et al. 2011, A&A, 527, 147
Mott, A., Spitoni, E., & Matteucci, F. 2013, MNRAS, 435, 2918
Nidever, D. L., Bovy, J., Bird, J. C., et al. 2014, ApJ, 796, 38
Portinari, L., & Chiosi, C. 2000, A&A, 355, 929
Romano, D., Chiappini, C., Matteucci, F., & Tosi, M. 2005, A&A, 430, 491
Rőskar, R., Debattista, V. P., Quinn, T. R., Stinson, G. S., & Wadsley, J. 2008, ApJL, 684, L79
Rőskar, R., Debattista, V. P., Quinn, T. R., & Wadsley, J. 2012, MNRAS, 426, 2089
Sackett, P. D. 1997, ApJ, 483, 103
Sánchez-Blázquez, P., Rosales-Ortega, F., Méndez-Abreu, J., et al. 2014, A&A, 570, A6
Scalo, J. M. 1986, FCPh, 11, 1
Schönrich, R., & Binney, J. 2009a, MNRAS, 396, 203
Schönrich, R., & Binney, J. 2009b, MNRAS, 399, 1145
Sellwood, J. A., & Binney, J. J. 2002, MNRAS, 336, 785
Smet, C., Posacki, S., & Ciotti, L. 2014, MNRAS, in press (arXiv:1412.4794)
Spitoni, E., & Matteucci, F. 2011, A&A, 531, A72
Spitoni, E., Matteucci, F., & Marcon-Uchida, M. M. 2013, A&A, 551, A123
van den Hoek, L. B., & Groenewegen, M. A. T. 1997, A&AS, 123, 305
Vera-Ciro, C., D'Onghia, E., Navarro, J., & Abadi, M. 2014, ApJ, 794, 173
Woosley, S. E., & Weaver, T. A. 1995, ApJ, 101, 181
Wyse, R. F. G., & Silk, J. 1989, ApJ, 339, 700